Assortative and disassortative mixing investigated using the spectra of graphs

Sarika Jalan[1,2] and Alok Yadav[1]

[1]*Complex Systems Lab, Indian Institute of Technology Indore, M-Block, IET-DAVV Campus, Khandwa Road, Indore 452017, India*

[2]*Centre for Biosciences and Biomedical Engineering, Indian Institute of Technology Indore, M-Block, IET-DAVV Campus, Khandwa Road, Indore 452017, India*

(Received 22 July 2014; revised manuscript received 17 October 2014; published 20 January 2015)

We investigate the impact of degree-degree correlations on the spectra of networks. Even though density distributions exhibit drastic changes depending on the (dis)assortative mixing and the network architecture, the short-range correlations in eigenvalues exhibit universal random matrix theory predictions. The long-range correlations turn out to be a measure of randomness in (dis)assortative networks. The analysis further provides insight into the origin of high degeneracy at the zero eigenvalue displayed by a majority of biological networks.

DOI: 10.1103/PhysRevE.91.012813 PACS number(s): 89.75.Hc, 02.10.Yn

I. INTRODUCTION

The past two decades have witnessed a rapid advancement in the field of complex networks [1–3]. The prime idea governing this framework is to consider a system made of interacting units. To categorize and understand real-world systems based on interacting units, many models have been proposed, among which the Erdös-Rényi (ER) random model [4], the scale-free (SF) model [5], and the small-world model [6] are the most popular. In addition, degree-degree correlations have also been used as one of the key properties of network characterization [2,7–18], and they are known to confer robustness to biological networks [19]. The tendency of (un)like degree nodes to stick together is termed (dis)assortativity. Various social networks are known to be assortative, while few of the biological and technological networks have been reported to be disassortative [13–18]. Despite its importance for real networks, (dis)assortativity does not appear in any of the model networks discussed above, and it is driven by some other mechanism, for example the reshuffling algorithm [20]. While the spectral behavior of uncorrelated networks has been quite well understood [21], despite real-world systems being highly correlated [9], such an understanding for the correlated networks still needs to be developed.

Spectral graph theory is an established branch of mathematics, and eigenvalues of corresponding adjacency matrices are known as fingerprints of the underlying graphs [22–25]. With recent advancement in the network theory, the spectral graph theory, traditionally used in investigations of random and regular graphs, got extended to studies of graphs motivated by real-world systems. These spectral studies, apart from presenting bounds for extremal eigenvalues, highlight their importance by relating them with the various structural as well as dynamical properties of the networks [26,27]. The studies of networks further reveal a key impact of assortativity on the extremal eigenvalues [28], which has been explored in the context of disease spreading [29] and diffusion processes [30], thereby exhibiting the importance of spectral studies of networks for a more comprehensive understanding of complex systems. This paper presents a systematic analysis of the impact of degree-degree correlations on the spectral properties of various networks under the random matrix theory (RMT) framework. Since its introduction in the 1960s, in the context of nuclear spectra, the theory has been successfully applied to a wide range of complex systems ranging from quantum chaos to a galaxy [31,32]. Recently, with a spurt in the activities of a network framework, the RMT was extended in an analysis of the spectral properties of various model networks [33,34] as well as those arising from real-world systems [35,36].

II. METHODS AND TECHNIQUES

To quantify the degree-degree correlations of a network, we consider the Pearson (degree-degree) correlation coefficient, given as [7,9]

$$r = \frac{\left[M^{-1}\sum_{i=1}^{M} j_i k_i\right] - \left[M^{-1}\sum_{i=1}^{M} \frac{1}{2}(j_i + k_i)^2\right]}{\left[M^{-1}\sum_{i=1}^{M} \frac{1}{2}\left(j_i^2 + k_i^2\right)\right] - \left[M^{-1}\sum_{i=1}^{M} \frac{1}{2}(j_i + k_i)^2\right]}, \tag{1}$$

where j_i,k_i are the degrees of nodes at both ends of the ith connection, and M represents the total connections in the network.

The random network of size N and average degree $\langle k\rangle$ is constructed using the ER model by connecting each pair of nodes with the probability $p = \langle k\rangle/N$ [4]. These networks have an assortativity coefficient (r) that is close to zero or exactly zero. To generate the networks with various assortativity, we use the reshuffling algorithm [20]. In this algorithm, after selecting two pairs of nodes randomly, we sort them according to degree. The highest degree node is then connected to the second highest degree node with the reshuffling probability p_r, which governs the (dis)assortative mixing, i.e., we reconnect a high degree node to a (low) high degree one and a low degree node to a (high) low degree one. With the probability $1 - p_r$, we rewire them randomly. If a new connection resulting from this rewiring already exists, it is discarded and the previous steps are performed. The process is carried out until a steady value of r is attained. For assortative networks, with the k degree nodes forming a complete graph with the value of r being 1, the network should have at least $(k + 1 + 2n)$ nodes, where n can be any integer starting from 0. As this condition is not satisfied for all the degrees present in the network, the network takes a value smaller than 1. Similarly, the disassortative network can have a value of r less than -1.0.

We note in addition that at high assortativity values, all the similar degree nodes that are connected among

themselves form groups [20]. As we decrease the assortativity, the connections within the groups of similar degree nodes decrease and the connections between different groups of similar degree nodes increase. For disassortative networks, connections between different groups of similar degree nodes exist, giving rise to a bipartite-like structure [20].

The SF networks of size N and average degree $\langle k\rangle$ are generated using the Barabási-Albert algorithm by starting with a completely connected network seed and adding new nodes one by one that connect with existing nodes using the preferential attachment method [1].

The networks are represented in the form of an adjacency matrix by defining $A_{ij} = 1$ if i and j nodes are connected, otherwise $A_{ij} = 0$. For an undirected and unweighted network with N nodes, the adjacency matrix is an $N \times N$ symmetric square matrix entailing all real eigenvalues. We denote the eigenvalues as λ_i, $i = 1,2,\ldots,N$ and $\lambda_i \leqslant \lambda_{i+1}$, and we analyze them under the RMT framework. The random matrix studies consider two properties of a spectra: (i) global properties such as spectral distribution of the eigenvalues $\rho(\lambda)$, and (ii) local properties such as eigenvalue fluctuations around $\bar{\lambda}$. In RMT, calculations of spectral fluctuations are done using the unfolded eigenvalues $\bar{\lambda_i} = \bar{N}(\lambda_i)$, where $\bar{N}(\lambda) = \int_{\lambda_{\min}}^{\lambda} \rho(\lambda')\, d\lambda'$ is the average integrated eigenvalue density [37]. By using these unfolded eigenvalues, nearest-neighbor spacings are calculated as $s_i = \bar{\lambda}_{i+1} - \bar{\lambda_i}$. For symmetric random matrices with mean 0 and variance 1, the nearest-neighbor spacing distribution (NNSD) follows Gaussian orthogonal ensemble (GOE) statistics given as

$$P(s) = \frac{\pi}{2} s \exp\left(-\frac{\pi s^2}{4}\right), \tag{2}$$

which shows a level repulsion at small spacing values with an exponential fall for larger spacings, indicating that nearest-neighbor eigenvalues are correlated [37]. In contrast, the spacing distribution of a matrix whose diagonal elements are Gaussian-distributed random numbers and the remaining elements are zero exhibit Poisson statistics [$P(s) = \exp(-s)$], indicating that eigenvalues are uncorrelated [37].

The intermediate of these two distributions can be characterized using the Brody equation [38]:

$$P_\beta(s) = A s^\beta \exp(-\alpha s^{\beta+1}), \tag{3}$$

where A and α are determined by the parameter β as $A = (1+\beta)\alpha$ and $\alpha = [\Gamma(\frac{\beta+2}{\beta+1})]^{\beta+1}$. The value of the Brody parameter lies in the range $(0 \leqslant \beta \leqslant 1)$. The value of β being 0 indicates the Poisson distribution, whereas $\beta = 1$ corresponds to the GOE distribution. Other values of β indicate that the distribution lies between these two.

The NNSD provides a correlation measure of subsequent eigenvalues, whereas the $\Delta_3(L)$ statistic measures how the eigenvalues that are L distance apart are correlated, and they can be estimated using the least-square deviation of the spectral staircase function representing the average integrated eigenvalue density $\bar{N}(\lambda)$ from the best fitted straight line for a finite interval of length L of the spectrum given by [32]

$$\Delta_3(L;x) = \frac{1}{L} \min_{a,b} \int_x^{x+L} [N(\bar{\lambda}) - a\bar{\lambda} - b]^2\, d\bar{\lambda}, \tag{4}$$

where a and b are regression coefficients obtained after a least-square fit. The average over several choices of x gives the spectral rigidity, i.e., $\Delta_3(L)$. For the GOE statistics, $\Delta_3(L)$ depends on L in the following manner:

$$\Delta_3(L) \sim \frac{1}{\pi^2} \ln L. \tag{5}$$

For the network spectra considered in this paper, there is no analytical form of $\bar{N}$, and we perform unfolding by numerical polynomial fitting using the smooth part of the spectra by discarding eigenvalues toward both ends as well as degenerate eigenvalues, if any [31,32]. This renders the dimension of the unfolded eigenvalues less than the dimension of the network.

III. RESULTS

The bulk part of the spectra of ER random networks with the value of r close to 0 follows the well-known semicircular law [39,40] [Fig. 1(f)]. The extremal eigenvalues deviate from the random matrix predictions and indeed provide various pieces of information about the structural and dynamical properties of corresponding systems [11,26,27,29,41]. In the following, we present results pertaining to the impact of assortativity on the spectral properties of networks. It turns out that with an increase in the assortativity, the semicircular distribution, as observed for the uncorrelated ER random networks, remains unchanged [Figs. 1(a)–1(e)]. The largest eigenvalue exhibits an increasing trend, as already discussed in [28,29]. As the network is rewired, entailing disassortativity, the spectral distribution [$\rho(\lambda)$] acquires a very different structure from those of the assortative networks. The networks start exhibiting a high degeneracy at zero, with the overall spectra resembling a double-humped structure [Fig. 1(h)], which becomes more pronounced as the disassortativity becomes higher or the value of r becomes more negative [Fig. 1(i)]. This increase in disassortativity is also accompanied with a larger number

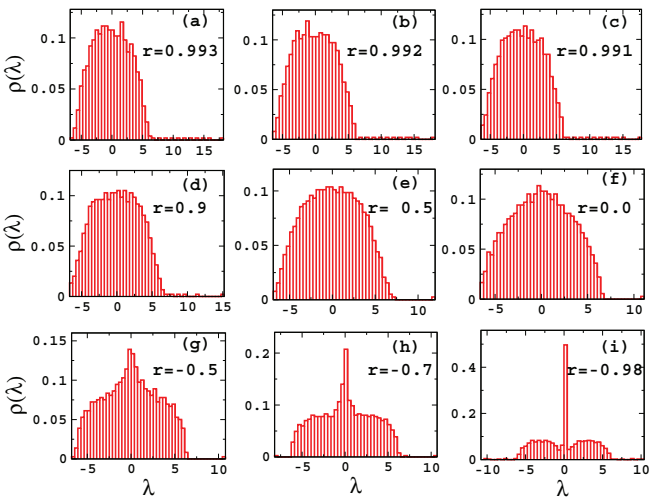

FIG. 1. (Color online) Spectral density for Erdös-Rényi random networks with different values of assortativity coefficient r. All graphs are plotted for the networks with size $N = 1000$ and connection probability $p = 0.01$, averaged over 20 different realizations of the networks.

of degenerate eigenvalues at zero. There could be various reasons for this high degeneracy. The few that are appropriate in the present context are as follows: First, as was discussed, disassortativity supports a bipartite-like structure [20], and a complete bipartite network has all zero eigenvalues except two. Hence the bipartite-like behavior of the disassortative networks is one of the reasons for the occurrence of high degeneracy at zero. Second, a treelike structure has been demonstrated to yield degeneracy at zero eigenvalue [42], and disassortativity encourages a treelike structure [20], which in turn indicates high degeneracy at zero. We remark that for large N, the limiting shape of $\rho(\lambda)$ is known for various cases, which for sufficiently dense matrices tend to follow the Wigner semicircular law typical for the Gaussian matrix ensembles [39,40], whereas an ensemble of sparse random matrices of finite size is known to yield states beyond the semicircular law in the tails of the distribution [43–45]. For sparse random graphs, i.e., matrices with 0 and 1 entries having smaller p values, while the density distribution $\rho(\lambda)$ of an ensemble exhibits singularities, with the height of the peaks being the corresponding multiplicities, the bulk is still shown to comply with random matrix predictions of Wigner's semicircular law [46,47]. Moreover, investigations of various model networks mimicking real-world properties have revealed that the spectra of these networks exhibit degeneracy at zero [37], as observed for the sparse random matrices. In that regard, despite the degeneracy at zero, it is not surprising that most of the assortative networks follow a semicircular distribution.

The spectral density only provides the global behavior of eigenvalues. Therefore, in order to get insight into local fluctuations, we further analyze the short-range and long-range correlations in eigenvalues. The NNSD follows GOE statistics of RMT [Eq. (2)] for all values of r except for very high values corresponding to the highly assortative networks (Fig. 2). What is interesting is that at the values of r for which $\rho(\lambda)$

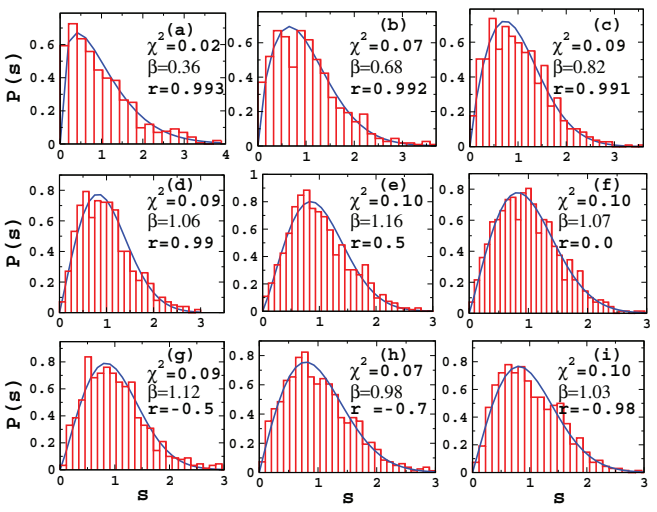

FIG. 2. (Color online) The NNSD for Erdös-Rényi random networks with different values of assortativity coefficient r. All graphs are plotted for the networks with size $N = 1000$ and connection probability $p = 0.01$. Histograms are from the data points, and the solid line is for fitting with the Brody distribution [Eq. (3)].

exhibits a very similar behavior, except for a change in the value of the largest eigenvalue, the NNSD captures crucial structural changes reflected through the value of the Brody parameter. For the highest achievable value of the assortativity coefficient for the particular network parameter for which results are presented, the value of β comes out to be close to 0.3 [Fig. 2(a)], and as the assortativity decreases, we witness a smooth transition to the GOE statistics with the value of β becoming 1. Depending on the network size, the average degree, and the degree sequences, the highest achievable value of r for that network may be different (as discussed in Sec. II), which might lead to a different value of β. Figures 1(a)–1(d) show that a very small change in the value of r is capable of entailing a profound change in the statistics; in fact, they change from Poisson statistics to GOE statistics. Since a very small randomness is known to be sufficient when introducing the short-range correlation in eigenvalues [48], a very small deviation from the highest assortativity entails GOE statistics. Since the assortativity in the network supports the groups having similar degree nodes, and as assortativity decreases, these distinct groups of nodes observed for very high values of r get destroyed, leading to a transition from Poisson to GOE statistics. As soon as the value of r is decreased, and sufficient random connections among the groups of similar degree nodes are induced, the value of the Brody parameter β becomes 1, and no further signature of structural changes to the value of β is found with a further decrease in the assortativity.

For disassortative networks that are characterized by negative values of r, what is remarkable is that despite these networks displaying spectral distributions distinguishable from those of the assortative networks, the NNSD yields the value of the Brody parameter ($\beta = 1$) bringing them into the universality class of GOE. This is not surprising as NNSD is analyzed by taking the nondegenerate part of the spectra, and high degeneracy at a particular value, for instance at zero, does not account for any effect in the NNSD. As long as the underlying network has some random connections, the NNSD displays GOE statistics [48]. We remark that all the networks considered here form a single connected cluster, because for disconnected networks, even though each individual subnetwork follows GOE statistics, the spectra taken together may lead to a different spacing statistics [33].

To gain further insight into the structural changes arising due to the changes in r values, we probe the long-range correlations in eigenvalues for those sets that yield a β value of 1. We find that for all these values of r, the long-range correlations, measured using the $\Delta_3(L)$ statistic [Eq. (4)], follow the universal GOE statistics as given by Eq. (5) for a certain value of L (denoted as L_0), and they deviate from this universality afterward (Fig. 3).

Note that a regular network, for instance a 1D lattice with a periodic boundary condition, follows a Poisson distribution. As connections are rewired, thereby increasing the randomness in the network, the value of the Brody parameter increases with an increase in the rewiring probability, and it becomes 1 at the onset of the small-world transition, demonstrating that nearest-neighbor eigenvalues are correlated [48]. For such a small change in the network structure, there is no visible change in the density distribution, but the Brody distribution detects even such a small change in the number of random

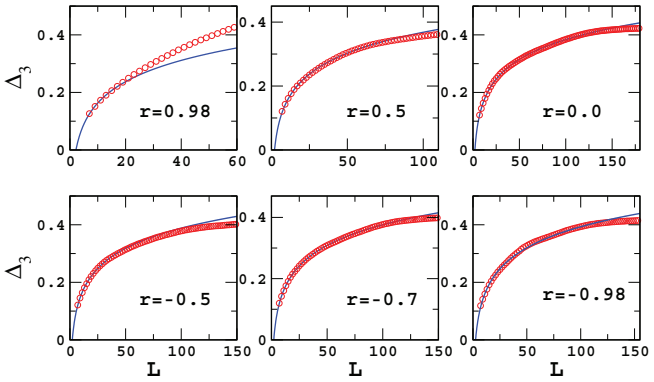

FIG. 3. (Color online) The $\Delta_3(L)$ statistic for Erdös-Rényi random networks with different values of assortativity coefficient r. All graphs are plotted for the networks with size $N = 1000$ and connection probability $p = 0.01$. The solid line is the prediction from GOE statistics [Eqs. (4) and (5)], and open circles are calculated from the network.

connections, and hence it has been proposed to be used as a measure of randomness at a fine scale [48]. After the Brody parameter attains a value of 1, the $\Delta_3(L)$ statistic has been shown to measure the randomness (in terms of L_0 in this paper) in the underlying network [49]. As the rewiring probability increases further, the value of L_0 for which the $\Delta_3(L)$ statistic follows RMT predictions increases, demonstrating that the eigenvalues that are L_0 distance apart are also correlated. Since L_0 provides a measure of randomness in a network [49], for the networks under investigation in the present work, it turns out that the highest assortative network is the least random, as the value of L_0 is the lowest for that particular r value [Fig. 3(a)]. As assortativity of the network is decreased, the randomness of the network increases, as reflected in the higher value of L_0. This increase in the size of L_0 continues up to r being 0, supporting the idea that the network reaches maximum randomness. The value of L_0 then remains steady for a further decrease in the value of assortativity to the smallest possible value of r, i.e., to the maximum disassortativity [Fig. 3(c)]. As most of the real-world networks have been reported to possess a certain level of disassortativity [9], based on the $\Delta_3(L)$ results, we can argue that real-world systems attempt to have more randomness, thereby leading to disassortativity. What follows is that as the value of r increases, by keeping the network size and the average degree the same, the value of L_0 for which the $\Delta_3(L)$ statistic follows RMT predictions increases, indicating an increased amount of randomness in the underlying network. Figure 4 demonstrates that the behavior of various spectral properties remains unchanged as the network size increases. Figures 4(a)–4(c) indicate that the value of the Brody parameter β becomes 1 with a very small decrease in the value of r. With a further decrease in the value of r, the value of L_0 for which the $\Delta_3(L)$ statistic follows the GOE statistic increases, indicating an increase in randomness, as discussed earlier. With a further decrease in the value of r in the disassortativity regime, there occurs a peak at zero eigenvalue that becomes more pronounced as the network becomes more dissociative, which is also accompanied by the deviation from the semicircular distribution at very low values of r.

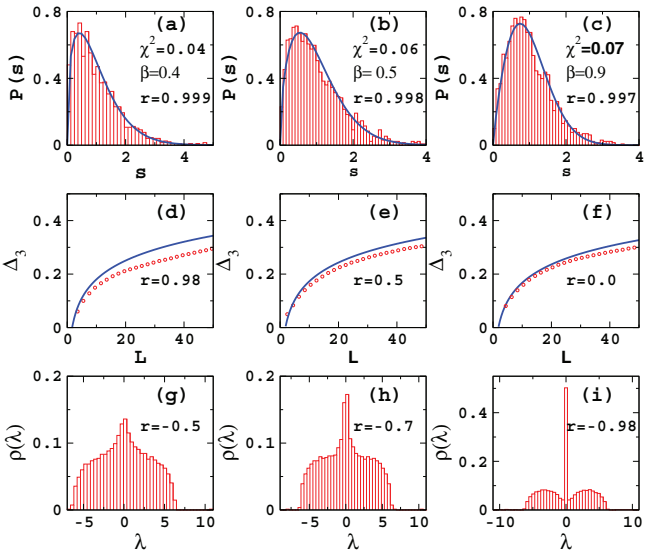

FIG. 4. (Color online) Parts (a)–(c) represent the NNSD, (d)–(f) represent the $\Delta_3(L)$ statistic, and (g)–(i) depict the spectral density distribution of ER random networks. All graphs are plotted for the networks with size $N = 2000$, $\langle k \rangle = 10$ and for the average over 20 different realizations of the network.

Further, in order to demonstrate the robustness of the universal RMT predictions against changes in the network architecture, we present results for the SF networks for various values of r. For r close to 0, the density distribution of the SF networks exhibits a triangular shape [40], which, with an increase in the assortativity, tends to display a flattening of the peak. The range of the distribution also shrinks as the assortativity increases [Figs. 5(a)–5(e)]. On the other hand, as we decrease assortativity, i.e., make the network more disassortative, the shape of the density distribution starts changing from its signature triangular distribution, with the peak at zero eigenvalue being more pronounced [Figs. 5(f) and 5(g)]. As we further increase the disassortativity, the

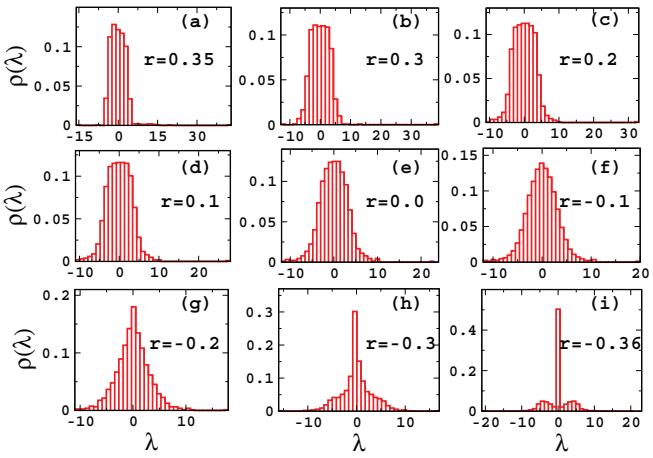

FIG. 5. (Color online) Spectral density for scale-free networks with different values of assortativity coefficient r. All graphs are plotted for the networks with size $N = 1000$, $\langle k \rangle = 10$ for 20 different realizations.

eigenvalues distribute themselves symmetrically and adopt a double-hump shape for highly disassortative networks, clearly visible in Fig. 5(i), which is accompanied by a high peak at the zero eigenvalue similar to that of the ER random networks. It is noteworthy that for highly disassortative networks, the spectral density of ER and SF model networks behaves similarly, deviating from their respective signature distributions. Further, the β value exhibits a transition from the Poisson to the GOE statistics with a decrease in the r value. Despite the overall spectral density being different from that of the ER networks, the NNSD and $\Delta_3(L)$ statistic display a similarity in behavior, which is in line with the argument that the eigenvalue fluctuations are calculated from the smooth homogeneous part of the spectra by not taking degeneracy into account, and density is not known to be a real test of GOE statistics [50].

We would like to remark here on the impact and reliability of network size considered in the present investigation. In RMT, different quantities are calculated by averaging an ensemble of matrices. However for real systems, calculations are made as running averages over part of the whole spectrum. The random matrix predictions can be applied to real-world systems if the above two are equivalent, a property known as ergodicity. More explicitly, it means that all members of the ensemble, except for a set of measure zero, satisfy the above equivalence [51,52]. Due to the ergodicity, one can construct matrix ensembles in different ways: (a) large dimensional random matrices with fewer realizations, or (b) smaller dimensional matrices with a larger number of realizations. We consider an ensemble of 20 network realizations with a large dimension, which is already shown to be good enough to study various structural properties of networks, such as degree distributions, clustering coefficients, etc. [6]. Moreover, individual entities of each ensemble follow RMT predictions for NNSD with good accuracy, characterized by χ^2 values. As we increase the realizations, accuracy increases (see Fig. 2 and the Appendix). Consideration of an ensemble consisting of many more network realizations would not lead to significant betterment or a difference in the following properties of the network spectra: (i) the Brody parameter smoothly turning 1 with a decrease in the value of r at a very fine scale; (ii) a further decrease in the values of r leading to an increase in the value of L for which spectra follow GOE statistics; and (iii) increasing height of the peak at zero eigenvalues with an increase in the disassortativity, due to the bipartite-like structure of the network.

Next, in order to investigate whether the degree-degree correlations in a real-world system have different spectral behavior from those of the model networks discussed above, we consider the protein-protein interaction (PPI) networks of six different species. These networks have already been shown to follow universal RMT predictions of GOE statistics [53]. We concentrate here on the occurrence of high degeneracy at the zero eigenvalue. The assortativity coefficient and the fraction of degenerate eigenvalues are tabulated in Table I. As all the PPI networks possess negative value of r as well as having a high degeneracy at zero, we expect disassortativity to be one of the factors governing the degeneracy in the real-world networks. To probe more into the correlation between disassortativity and degeneracy at zero, we compare the corresponding configuration model for all PPI networks presented above (Table I). It is clearly indicated that as soon as the value of r becomes negative (close to the corresponding PPI network), while keeping all other parameters of the system the same, there is an increase in the degeneracy at zero eigenvalue.

TABLE I. Comparison of the number of zero eigenvalues of PPI networks of different species and their corresponding configuration models. r_0 denotes the value of the assortativity coefficient for the PPI networks. N_0 (PPI) denotes the number of zero eigenvalues in the spectra of the PPI networks. N_0 ($r = 0$) stands for zero degeneracy for the configuration model with $r = 0$, whereas N_0 ($r = r_0$) denotes the same for the configuration models taking r values equal to the corresponding PPI network.

PPI networks	N	r_0	N_0 (PPI)	N_0 ($r = 0$)	N_0 ($r = r_0$)
H.pylori	709	−0.243	317	115	152
C.elegans	2386	−0.183	1354	465	1124
S.cerevisiae	5019	−0.088	976	717	1149
H.sapiens	2138	−0.084	864	423	643
D.melanogaster	7321	−0.083	2311	1389	1975
E.coli	2209	−0.012	487	487	497

IV. DISCUSSION AND CONCLUSIONS

The density distribution of the random networks for the value of r being 0 follows the Wigner semicircular distribution. Even with a change in the assortativity ($0 \leqslant r < 1$), the bulk part of the spectra keeps displaying a semicircular distribution [Figs. 1(a)–1(f)], whereas an increase in the disassortativity ($-1 \leqslant r < 0$) leads to a double hump, which is symmetrically distributed around a peak at zero eigenvalue [Fig. 1(i)]. The height of the peak increases with an increase in the disassortativity of the network.

The NNSD of the networks with the various (dis)assortativity values ($1 < r < -1$) reveals that there is a smooth transition in the β-value around the very high assortativity regime. For very high assortativity values, β values lie close to 0, and as the network becomes less assortative, β progresses to 1. This may be because the networks with the highest assortativity has groups of similar degree nodes that get perturbed as r decreases by making random connections among these different groups. For the rest of the assortativity values, β remains fixed at 1, which corresponds to the universal GOE distribution as the value of r becomes negative.

Furthermore, the property of the Brody parameter being able to detect changes in the network structure at a fine scale, and the increase in L_0 of the $\Delta_3(L)$ statistic after the value of β becomes 1, have several implications. The implication that pertains to the present work is that the value of β distinguishes two networks based on the random connections present, while the other implication is that more assortativity in the network corresponds to less randomness. Decreasing the assortativity leads to an increase in randomness, which continues up to the value of $r = 0$, for which the network is most random (the L_0 value being maximum). Then the value of L for which the $\Delta_3(L)$ statistic follows the GOE prediction starts decreasing and remains steady for a further decrease in the value of assortativity up to the lowest possible value of r (i.e.,

up to the maximum disassortativity case). The SF networks also exhibit eigenvalue fluctuation statistics similar to those for ER random networks, where the density distribution for $r = 0$ and for lower $|r|$ values exhibits a triangular instead of a semicircular shape. Both networks, however, exhibit high degeneracy at zero for the disassortative networks. By considering different PPI networks, we further demonstrate the role of disassortativity governing the appearance of degeneracy at zero eigenvalue.

In spectral graph theory, most of the works concentrate on extremal eigenvalues [22], whereas RMT research focuses on the distribution of various spectral properties of random matrices with an extension to random graphs, largely ignoring many graph properties that exist in real-world systems. The analysis carried out here is a step toward bridging this gap by considering the two most popular tools of random matrix theory, i.e., density and spacing distributions, in order to understand the impact of one of the important properties of graphs, i.e., assortativity. This property has been increasingly realized as a characteristic of a system [54–56]. Our analysis is another demonstration of the importance of spacing analysis in understanding the impact of degree-degree correlation on a network detected through the spectra, as for very minute changes in r there are no visible changes in the spectral density. However, this leads to very drastic changes in eigenvalue fluctuations, demonstrating the impact of r values on randomness in a network.

Furthermore, the $\Delta_3(L)$ statistic provides insight into why social networks tend to be assortative while biological and technological networks tend to be disassortative, as randomness, measured in terms of L_0 for which the $\Delta_3(L)$ statistic follows the RMT prediction, increases with a decrease in r. A direct implication of this result can be seen in the case of social networks, where entities are known to be associated in an ordered fashion (people with similar ages or educational profiles are often more connected) [57], thus providing a probable reason as to why social networks tend to assume an assortative topology. On the other hand, it has been reported that most biological and technological networks possess a certain level of disassortativity [7,9,18]. Also, biological networks, e.g., PPI networks, exhibit varying amounts of randomness in their underlying networks detected through different values of L_0 for which the $\Delta_3(L)$ statistic follows GOE statistics [53]. This randomness has been attributed to mutations occurring over the course of evolution [58]. Relating the disassortative nature of the PPI networks and the randomness they possess with the results obtained from our analysis of the model networks suggests that biological networks tend to become more disassortative in order to comply with their underlying randomness.

To conclude, we present a systematic analysis of the spectral properties of networks with varying (dis)assortativity. We find that assortativity has a profound impact on the spectral properties of the underlying networks. At a very high assortativity regime, even with a slight decrease in the value of r, the Brody parameter smoothly becomes 1. A further decrease in the values of r leads to an increase in the value of L_0 of the $\Delta_3(L)$ statistic for which the spectra follow GOE statistics. The Brody parameter β captures the changes in the assortativity coefficient at a fine scale [48] and L_0 at a large scale [49], which further suggests that when r decreases, randomness increases. With a further decrease in r, at around $r = 0$, the density distribution starts exhibiting a peak at zero eigenvalue, which becomes more pronounced as r decreases further. Interestingly, most of the studies on network spectra report that the bulk part of the spectra of the networks with a Gaussian and scale-free degree distribution follow semicircular and triangular distributions [39,40], respectively, but for highly disassortative networks, the spectral density of both degree distributions can have entirely different behavior.

Recently, the realm of assortativity has been realized in understanding adaptive synchronization [55], which, combined with our results of varying the amount of randomness for various values of r, can be explored further to understand the dynamical processes in networks. Furthermore, Table I indicates that disassortativity is one of the factors contributing to zero degeneracy. The prevalence of zero degeneracy has been implicated in terms of gene duplication [59]. This, along with the impact of a change in the topology of a network brought about by assortativity, leading to a profound change in the spectral density, provides a direction in which to explore the evolutionary origin of real-world systems [60,61]. Lastly, since randomness or random connections in a network have already been emphasized for the proper functioning of corresponding systems [62], the profound role of the assortativity parameter revealed through the sophisticated random matrix technique is not only important for a network community attempting to model complex systems, but it is interesting for random matrix communities at the fundamental level as well.

ACKNOWLEDGMENTS

S.J. thanks the Department of Science and Technology (DST), Government of India Grant No. SR/FTP/PS-067/2011, and the Council of Scientific and Industrial Research (CSIR), Government of India Grant No. 25(0205)/12/EMR-II for funding. It is a pleasure to acknowledge Kunal Bhattacharya

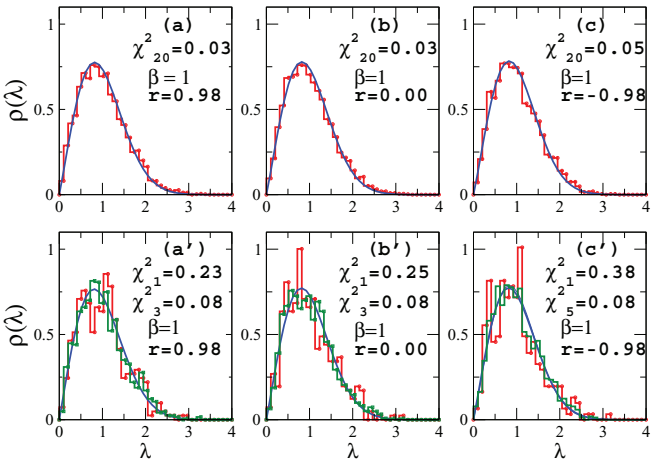

FIG. 6. (Color online) Parts (a), (b), and (c) plot the average NNSD for an ensemble of 20 realizations for different values of r, whereas (a′), (b′), and (c′) plot the ensemble having a different number of the network realizations. The histogram is drawn using the data from the networks, and the solid line is the fitted Brody distribution. For all the graphs, $N = 1000$ and $\langle k \rangle = 10$.

(BITS PILANI) and Igor M. Sokolov (Humboldt-Universität zu Berlin) for help with Sokolov's algorithm. A.Y. acknowledges Council of Scientific and Industrial Research (CSIR), Government of India for financial support.

APPENDIX

Numerical calculations pertaining to assortative mixing, eigenvalues calculations, and $\Delta_3(L)$ statistics are done using FORTRAN code written by the authors. The eigenvalues are calculated by calling LAPACK (Linear Algebra PACKage) subroutines into the FORTRAN code. The calculation of spacings and polynomial fittings are done using MATLAB.

We present the χ^2 values as a measure of the goodness of fit of the model to data, with a lower value of χ^2 indicating a better fitting. As depicted in Fig. 6, the χ^2 values consistently decrease with an increase in the number of network realizations in the ensemble, implicating an increase in accuracy up to the value of χ^2 being less than 1 lying in the acceptable range [63]. For assortative networks, as few as three realizations in the individual ensemble are sufficient to bring χ^2 within the acceptable range, whereas for r taking negative values, the number of realizations in the ensemble increases a bit more [five as depicted in Fig. 6(c)] in order to bring χ^2 within the acceptable range. This happens because for disassortative networks, there is high degeneracy at zero eigenvalue leading to a less effective dimension of the unfolded spectra (refer to discussions in Sec. II), and hence more realizations of the networks are required.

[1] R. Albert and A.-L. Barabási, Rev. Mod. Phys. **74**, 47 (2002).
[2] S. Boccaletti, V. Latora, Y. Moreno, M. Chavez, and D. U. Hwang, Phys. Rep. **424**, 175 (2006).
[3] A.-L. Barabási and Z. N. Oltvai, Nat. Rev. Genet. **5**, 101 (2004).
[4] P. Erdös and A. Rényi, Publ. Math. Debrecen **6**, 290 (1959).
[5] A.-L. Barabasi and R. Albert, Science **286**, 509 (1999).
[6] D. J. Watts and S. H. Strogatz, Nature (London) **393**, 440 (1998).
[7] M. E. J. Newman, Phys. Rev. Lett. **89**, 208701 (2002).
[8] M. T. Rivera, S. B. Soderstrom, and B. Uzzi, Annu. Rev. Sociol. **36**, 91 (2010).
[9] M. E. J. Newman, Phys. Rev. E **67**, 026126 (2003).
[10] M. Barthélemy, Europhys. Lett. **63**, 915 (2003).
[11] M. E. J. Newman, SIAM Rev. **45**, 167 (2003).
[12] V. Colizza, A. Flammini, M. A. Serrano, and A. Vespignani, Nat. Phys. **2**, 110 (2006); R. Cohen and S. Havlin, Phys. Rev. Lett. **90**, 058701 (2003); S. N. Soffer and A. Vázquez, Phys. Rev. E **71**, 057101 (2005).
[13] K. I. Goh, E. Oh, B. Kahng, and D. Kim, Phys. Rev. E **67**, 017101 (2003); M. Catanzaro, G. Caldarelli, and L. Pietronero, *ibid.* **70**, 037101 (2004).
[14] M. E. J. Newman and J. Park, Phys. Rev. E **68**, 036122 (2003); D. Lusseau and M. E. J. Newman, Proc. R. Soc. London, Ser. B **271**, S477 (2004).
[15] D. P. Croft, R. James, A. J. W. Ward, M. S. Botham, D. Mawdsley, and J. Krause, Oecologia **143**, 211 (2005).
[16] J. Bollen, B. Gonçalves, G. Ruan, and H. Mao, Artificial Life **17**, 237 (2011).
[17] G. Bagler and S. Sinha, Bioinformatics **23**, 1760 (2007).
[18] D. S. Bassett, E. Bullmore, B. A. Verchinski, V. S. Mattay, D. R. Weinberger, and A. M.-Lindenberg, J. Neurosci. **28**, 9239 (2008).
[19] D. A. Pechenick, J. L. Payne, and J. H. Moore, PLoS Comput. Biol. **10**, e1003780 (2014).
[20] R. Xulvi-Brunet and I. M. Sokolov, Phys. Rev.E **70**, 066102 (2004); Acta Phys. Pol. B **36**, 1431 (2005).
[21] J. Berg and M. Lässig, Phys. Rev. Lett. **89**, 228701 (2002).
[22] P. Van Meighem, *Graph Spectra for Complex Networks* (Cambridge University Press, Cambridge, 2011).
[23] G. Akemann, J. Baik, and P. D. Francesco, *The Oxford Handbook of Random Matrix Theory* (Oxford University Press, Oxford, 2011).
[24] F. R. K. Chung, *Spectral Graph Theory* (American Mathematical Society, USA 1997).
[25] D. Cvetković, P. Rowlinson, and S. Simić, *An Introduction to the Theory of Graph Spectra* (Cambridge University Press, Cambridge, 2010).
[26] P. Van Mieghem, J. Omic, and R. E. Kooij, EIRE/ACM Trans. Netw. **17**, 1 (2009).
[27] J. G. Restrepo, E. Ott, and B. R. Hunt, Phys. Rev. E **71**, 036151 (2005).
[28] P. Van Meighem, H. Wang, X. Ge, S. Tang, and F. A. Kuipers, Eur. Phys. J. B **76**, 643 (2010).
[29] A. V. Goltsev, S. N. Dorogovtsev, J. G. Oliveira, and J. F. F. Mendes, Phys. Rev. Lett. **109**, 128702 (2012).
[30] G. DÁgostino, A. Scala, V. Zlatić, and G. Caldarelli, Europhys. Lett. **97**, 68006 (2012).
[31] T. Guhr, A. M.- Groeling, and H. A. Weidenmüller, Phys. Rep. **299**, 189 (1998).
[32] T. Papenbrock and H. A. Weidenmüller, Rev. Mod. Phys. **79**, 997 (2007).
[33] G. Palla and G. Vattay, New J. Phys. **8**, 307 (2006).
[34] S. Jalan and J. N. Bandyopadhyay, Phys. Rev. E **76**, 046107 (2007).
[35] R. Potestio, F. Caccioli, and P. Vivo, Phys. Rev. Lett. **103**, 268101 (2009).
[36] S. Jalan, C. Sarkar, A. Madhusudanan, and S. K. Dwivedi, PloS One **9**, e88249 (2014).
[37] M. L. Mehta, *Random Matrices*, 2nd ed. (Academic, New York, 1991).
[38] T. A. Brody, Lett. Nuovo Cimento **7**, 482 (1973); T. A. Brody, J. Flores, J. B. French, P. A. Mello, A. Pandey, and S. S. Wong, Rev. Mod. Phys. **53**, 385 (1981).
[39] I. J. Farkas, I. Derényi, A.-L. Barabási, and T. Vicsek, Phys. Rev. E **64**, 026704 (2001).
[40] M. A. M. de Aguiar and Y. Bar-Yam, Phys. Rev. E **71**, 016106 (2005).
[41] H. Sompolinsky, A. Crisanti, and H. J. Sommers, Phys. Rev. Lett. **61**, 259 (1988); K. Rajan and L. F. Abbott, *ibid.* **97**, 188104 (2006); R. M. May, Nature (London) **238**, 413 (1972); S. Chauhan, M. Girvan, and E. Ott, Phys. Rev. E **80**, e056114 (2009).
[42] S. N. Dorogovtsev, A. V. Goltsev, J. F. F. Mendes, and A. N. Samukhin, Phys. Rev. E **68**, 046109 (2003).

[43] G. J. Rodgers and A. J. Bray, Phys. Rev. B **37**, 3557 (1988).
[44] Y. V. Fyodorov and A. D. Mirlin, J. Phys. A **24**, 2219 (1991).
[45] S. N. Evangelou, J. Stat. Phys. **69**, 361 (1992).
[46] T. Rogers, I. P. Castillo, R. Kühn, and K. Takeda, Phys. Rev. E **78**, 031116 (2008).
[47] I. Dumitriu and S. Pal, Ann. Probab. **40**, 2197 (2012).
[48] J. N. Bandyopadhyay and S. Jalan, Phys. Rev. E **76**, 026109 (2007).
[49] S. Jalan and J. N. Bandyopadhyay, Europhys. Lett. **87**, 48010 (2009).
[50] A. Pandey and M. L. Mehta, Commun. Math. Phys. **87**, 449 (1983).
[51] O. Bohigas and M. J. Giannoni, Ann. Phys. (NY) **89**, 393 (1975).
[52] J. B. French, P. A. Mello, and A. Pandey, Phys. Lett. B **80**, 17 (1978).
[53] A. Agrawal, C. Sarkar, S. K. Dwivedi, N. Dhasmana, and S. Jalan, Physica A **404**, 359 (2014).
[54] J. N. Tenenbaum, S. Havlin, and H. E. Stanley, Phys. Rev. E **86**, 046107 (2012).
[55] V. Avalos-Gaytán, J. A. Almendral, D. Papo, S. E. Schaeffer, and S. Boccaletti, Phys. Rev. E **86**, 015101(R) (2012).
[56] F. Papadopoulos, M. Kitsak, M. A. Serrano, M. Boguná, and D. Krioukov, Nature (London) **489**, 537 (2012).
[57] J. A. Smith, M. McPherson, and L. S.-Lovin, Am. Sociol. Rev. **79**, 432 (2014).
[58] D. A. Petrov, Genetica **115**, 81 (2002).
[59] S. A. Teichmann and M. M. Babu, Nat. Gen. **36**, 492 (2004).
[60] C. B. Victoria, T. Smieszek, H. Jianping, G. Cao, J. J. Rainey, H. Gao, A. Uzicanin, and M. Salathé, PloS One **9**, e87042 (2014).
[61] J. Alstott, S. Madnick, and C. Velu, PloS one **9**, e95140 (2014).
[62] G. Longo and M. Montévil, *Computation, Physics and Beyond* (Springer-Verlag, Berlin, Heidelberg, 2012), Vol. 7160, p. 289.
[63] M. C. Seiler and F. A. Seiler, Risk Anal. **9**, 415 (1989).